

SELECTION OF OPTIMAL TECHNOLOGICAL PARAMETERS FOR FORMING NOMINALLY FLAT SURFACES WITH LUBRICATING MICROCAVITIES

**Viktor P. Kuznetsov¹, Igor V. Tatarintsev²,
Vladimir V. Voropaev², Andrei V. Korelin¹**

¹Ural Federal University, Russia

²Kurgan State University, Russia

ORCID iDs: Viktor P. Kuznetsov
Igor V. Tatarintsev
Vladimir V. Voropaev
Andrei V. Korelin

<https://orcid.org/0000-0001-8949-6345>
<https://orcid.org/0009-0008-3303-0851>
<https://orcid.org/0000-0001-8508-073X>
<https://orcid.org/0000-0003-0650-2805>

Abstract. *This article demonstrates a multi-step process for forming a nominally flat surface with circumferential lubricating microcavities on a tribological assembly of an X38CrSi steel shaft. The process includes finish turning, preliminary strengthening burnishing, deformation profiling of microcavities by a honing stone and smoothing of microprotrusions. The study determines the optimal technological parameters for each of the transitions based on microhardness and oil absorption power maximization, as well as roughness and periodic impact minimization. The process optimization is conducted using the Taguchi experiment design method. The optimal combination of technological parameters for hardening burnishing was discovered to be: normal force $F = 200\text{ N}$; feed rate $f = 0.025\text{ mm/rev}$ and three tool passes. These burnishing parameters practically eliminate the influence of periodic impacts at spatial frequencies determined by the tool feed rate and the number of spindle rotations during turning. We determined suitable honing stone grit parameters and application force that yield microcavities 3.8 to $8.1\text{ }\mu\text{m}$ in depth, as well as the optimal parameters for smoothing of microprotrusions, resulting in a bearing area roughness of $S_a = 0.15\text{ }\mu\text{m}$ and oil absorption power of $13.74 \cdot 10^{-5}\text{ mm}^3/\text{mm}^2$.*

Key words: *Nominally flat surface, Lubricating microcavities, Burnishing, Deformation profiling, Microhardness, Roughness*

Received: December 15, 2023 / Accepted February 09, 2024

Corresponding author: Vladimir Voropaev

Kurgan State University, 640020, Sovetskaya st. 63, building 4, Kurgan, Russia

E-mail: sen_vvv@mail.ru

1. INTRODUCTION

Increasing the wear resistance of precision surfaces of tribological assembly parts remains an important technological challenge. One possible solution is controlling mechanical machining process modes to reduce the surface's roughness and increase its microhardness. Additional machining operations can be applied to increase the oil absorption power of the surface, methods for the formation of nominally flat surfaces with lubricating microcavities. Such methods are implemented by mechanical and physical machining.

In a review article, Pawlus et al. [1] analyzed methods for producing nominally flat surfaces with microcavities for liquids. Koszela et al. [2] describe a technology for the formation of oil-retaining microtopography on flat surfaces of tribological assemblies by finish milling and subsequent eccentric burnishing. Lubricating microcavities (oil pockets) are created in the form of dimples by steel and ceramic balls. The depth of cavities is 5 to 13 μm , their diameter is 0.15 to 0.33 mm. Mezghani et al. [3] proposed a method for obtaining a nominally flat surface with microcavities 4 to 6 μm in depth and 50 to 100 μm in width, by using a cylinder tool with honing stones. Zhang et al. [4] studied the formation of a surface with lubricating microcavities up to 5 μm in depth, obtained by using laser ablation.

Both particular parameter values and a multitude of surface topography parameters can be used to assess the quality of nominally flat surfaces and their tribological properties. Molnar [5] demonstrated that tribological properties of a surface can be characterized by the following 3D roughness parameters: maximum peak height – S_p , maximum valley depth – S_v , peak material volume – V_{mp} , valley void volume – V_{vv} , skewness – S_{sk} and kurtosis – S_{ku} . It was found that low values of the maximum peak height (S_p) and the functional-volumetric parameter (V_{mp}) provide for a higher wear-resistance of a surface, and a higher V_{vv} value indicates the increase of the surface's oil absorption power. Moreover, Molnar [6] uses a comprehensive analysis of height and functional parameters to determine the impact of topography on wear-resistance. It was established that a simultaneous reduction of S_{pk} and S_{sk} parameters to negative values leads to a better wear-resistance of the sample. Nadolny [7] studied the flatness parameters FL_{Tt} , FL_{Tp} , FL_{Tv} , FL_{Tq} and roughness parameters S_a , S_t , S_q , S_p , S_v after a three-step mechanical machining by milling, grinding, and burnishing. This study showed a stable correlation between flatness and roughness parameters.

Kuznetsov et al. [8] proposed a technology for highly productive formation of nominally flat oil-retaining microtopographies on surfaces of shafts by using multi-step machining within one setup on a CNC machine, consisting of, consequently: finish turning, preliminary hardening burnishing, production of lubricating microcavities by a special tool equipped with a self-aligning honing stone and finish smoothing burnishing.

Preliminary hardening burnishing allows one to simultaneously attain submicronic roughness and maximum load bearing capability. Thereafter, a special tool equipped with a self-aligning honing stone is used to produce lubricating microcavities of needed depth and oil absorption power by selecting the honing stone grit and its application force. The finish smoothing burnishing by a spherical indenter with a ≥ 6 mm radius removes protrusions created by the deformation profiling of lubricating microcavities. To effectively implement a multi-step machining procedure of this kind, careful optimization of the operating parameters is necessary to achieve the desired end result and reduce harmful interference between steps. The optimization is carried out based on orthogonal arrays proposed by G. Taguchi, which has seen extensive use as an optimization method. This technique allows for discovering systematic, simple and efficient solutions, minimizing the effort needed to achieve the desired result [9].

For example, this method is used for optimizing drilling [10-11] and turning [12] parameters. This method was also successfully used for studying and predicting characteristics of a surface layer of construction steels after nanostructuring burnishing [13-14].

For evaluating surface quality, power spectral density (PSD) analysis is a flexible mathematical tool, that is especially useful for identifying the influence of periodic impacts with different spatial frequencies during surface machining. This parameter is used to analyze functional surface properties in problems of contact mechanics, adhesion and thermal conductivity [15]. Use of PSD-analysis in contact mechanics was studied by Peresadko et al [16]. Surface roughness may have essential influence on the contact stiffness [17] and wear properties of contacting materials [18]. Popov and Pohrt [19] presented an evaluation of the PSD function spectra after ball milling, burnishing and finishing using a honing stone. It was discovered that a PSD function spectrum has five main constituents, varying in amplitude and wavelength. The appearance of said constituents correlates with periodical phenomena that occur in the mechanical machining system during the milling process. The dominating peak has a wavelength of 0.05 mm, corresponding to the milling feed value of 0.04 mm/tooth. The emergence of a peak with a wavelength of 0.26 mm, which is the first harmonic of the dominating peak, can be attributed to the formation of overlap traces. The PSD function spectrum also includes periodical components, whose wavelength does not correlate with the kinematics of the process. These components can be attributed to dynamic impacts in the machining system, removal mechanisms, or chip segmentation.

Only one dominant component of the PSD function that influences the forming of the surface texture was discovered during the burnishing process. Periodic impact has a significantly lower stepover than the burnishing feed of 0.02 mm. It is presumed that this impact is connected with the traces of plastic deformation of the material. The frequencies of PSD function peaks for surfaces after grinding are also different from those achieved during the milling process. It was discovered that milling traces do not get covered by burnishing traces, thus confirming the optimal and correct choice of technological parameters for burnishing of AlCu4MgSi alloy curved surfaces.

Martins et al. [20] used PSD analysis to investigate the influence of periodic feed rate impacts during turning and subsequent deep rolling at different tool contact pressures. It was found that at the lowest deep rolling feed rate of 0.06 mm/rev, the roughness peaks after the previous turning have a larger amplitude than at higher feed rates. Increasing the deep rolling feed rate to 0.09 and 0.12 mm/rev reduces the influence of prior turning. It was determined that at the lowest deep rolling feed rate, peaks with a wavelength of 0.06 mm (spatial frequency 16.667 mm^{-1}) are present on the PSD function, which correspond to the deep rolling feed rate. It was demonstrated that in case the deep rolling pressure increases, the turning feed peaks presented on the power spectral density function become almost invisible. Increasing the pressure and consequently the intensity of surface plastic deformation favors the concentration of peaks associated with the feed rate of turning, eliminating the peaks formed during the previous turning process. Hardening with a higher feed rate of 0.15 mm/rev further increases the amplitude of the peaks in the PSD function plot. Using the lowest feed rate during deep rolling results in more complex surface deformation and a series of peaks with a large spatial distribution.

The aim of this study is to determine the optimal combination of technological parameters for hardening burnishing (normal force, feed rate and number of tool passes) according to the criteria of microhardness HV, mean absolute error of microprofile Sa and the minimization of periodic impacts' influence that appear after the turning step, the optimization of grit and

application force of the honing stone during deformation profiling of lubricating microcavities by the criterion of surface oil absorption power, and normal force during smoothing burnishing by the criterion of minimum plateau roughness and maximum surface oil absorption power V_{vv} .

2. MATERIALS AND RESEARCH METHODS

As a sample tribological assembly part, we used a cylindrical workpiece 23 mm in diameter and 150 mm long, made of X38CrSi (C 0.37%; Cr 1.34%; Si 1.1%; Mn 0.47%; Cu 0.21%; Ni 0.05%; S 0.024%; P 0.019%) steel with hardness of 440 HB after oil quenching at a heating temperature of 900°C and tempering at 320°C with air cooling. We selected this material because of our efforts to increase the wear resistance of the shaft surface that is in contact with the needle bearing in the Burlak snow and swamp-going vehicle's transmission. The multi-step technology for the formation of nominally flat microtopography with lubricating microcavities on a CNC turning machining center Okuma/Genos L300M (Japan) under consideration consists of four consecutive processing step: finish turning and pre-burnishing, deforming profiling of microcavities and smoothing burnishing. Finish turning was carried out using a ZCC WNMG080408 cutting plate at a feed rate of $f_f=0.05$ mm/rev and the spindle speed of 1,650 rpm. After finish turning the microhardness value was 496 ± 9 HV_{0.05}.

Hardening burnishing was performed using a diamond tool of spherical shape with a radius of $R=2$ mm. Deforming profiling of lubricating microcavities was done with a special tool with a honing stone 20 mm in length and 4 mm in width. The work surface grit was 160/125 and 200/250. The final smoothing burnishing was carried out using a tool with a diamond spherical indenter with a 6 mm radius. Examples of workpiece machining by burnishing and deforming profiling of lubrication microcavities are shown in Fig. 1. To analyze the topography of the processed surfaces, we used a Wyko-NT1100 optical profilometer and Wyko Vision, Matlab, Gwyddion and MountainMap software. To measure microhardness, we used the AHOTEC Eco HARD XM1270C microhardness tester.

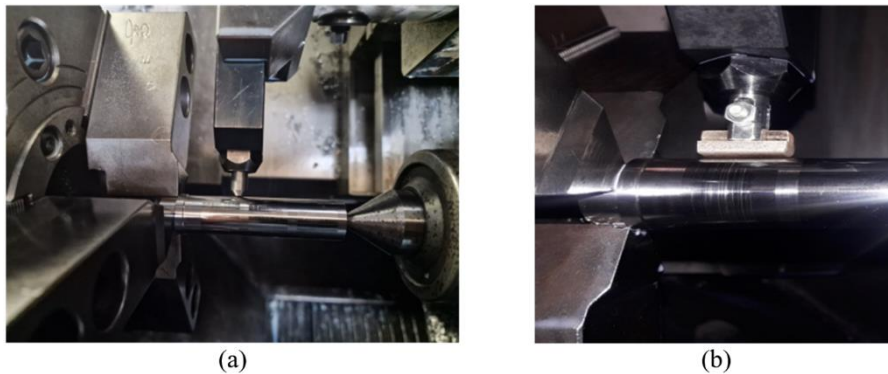


Fig. 1 Examples of workpiece surface machining by burnishing (a) and deforming profiling of microcavities using a tool with a honing stone (b)

3. EXPERIMENTAL RESEARCH

3.1. Finish Turning

After finish turning, the microprofile's arithmetic mean deviation (average roughness parameter) was measured at $S_a=443$ nm. Surface morphology and profilogram after turning are shown in Fig. 2. Using an optical profilometer with the WYKO Vision software, we determined the surface's oil absorption power to be $V_{vv}=6.95 \cdot 10^{-5}$ mm³/mm² after turning.

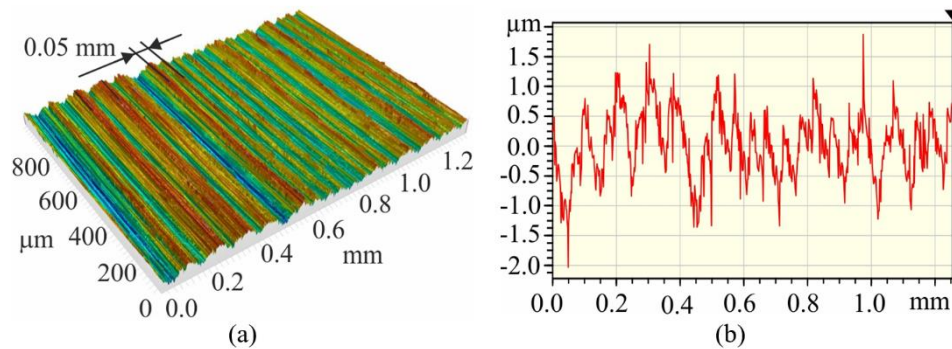


Fig. 2 Surface morphology (a) and profilogram (b) after finish turning

The surface spectrum after turning is influenced by two periodic peaks, as determined by power spectral density (PSD) estimation (Fig. 3). The first peak has a spatial frequency of $\omega_e=1.147$ mm⁻¹, a period of $t_e=0.8$ mm, and is related to spindle rotation speed of $n=1,650$ rev/min. The second peak has a spatial frequency of $\omega_t=19.463$ mm⁻¹ and corresponds to the turning feed rate $f_t=0.05$ mm/rev.

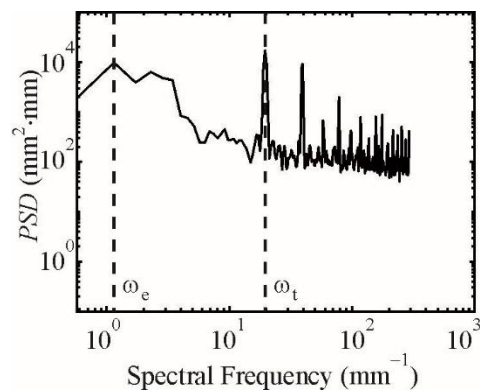


Fig. 3 Surface PSD function after finish turning

Periodical frequency PSD function components at frequencies higher than ω_t are believed to be connected to the geometry of the turning plate [18].

3.2. Determination of Optimal Pre-burnishing Parameters Using Taguchi Method

Further, to determine the optimal combination of preliminary strengthening burnishing parameters, we utilized the Taguchi method with an orthogonal array L9 and three levels of process parameters: burnishing force F , feed rate f and number of tool passes n_p . Based on the experimental studies of the process, we determined the optimal parameters for hardening burnishing to maximize microhardness $HV_{0.05}$. The study determined the correlation between pre-burnishing parameters and the arithmetic mean deviation of the microprofile of the surface area S_a . Table 1 shows the mean microhardness values $HV_{0.05}$ and arithmetic mean deviation of the S_a profile over five measurements.

Table 1 Machining modes and results

Exp. No	Altered parameter			$HV_{0.05}$	S_a (nm)
1	$F = 150$ N	$f = 0.01$ mm/rev	$n_p = 1$	623	147.6
2	$F = 150$ N	$f = 0.025$ mm/rev	$n_p = 2$	602.8	82.74
3	$F = 150$ N	$f = 0.04$ mm/rev	$n_p = 3$	595	68.03
4	$F = 200$ N	$f = 0.01$ mm/rev	$n_p = 2$	642.6	161.33
5	$F = 200$ N	$f = 0.025$ mm/rev	$n_p = 3$	657.4	73.35
6	$F = 200$ N	$f = 0.04$ mm/rev	$n_p = 1$	592.6	96.46
7	$F = 250$ N	$f = 0.01$ mm/rev	$n_p = 3$	584.2	440.06
8	$F = 250$ N	$f = 0.025$ mm/rev	$n_p = 1$	630.4	109.96
9	$F = 250$ N	$f = 0.04$ mm/rev	$n_p = 2$	615.8	90.53

We used MiniTab 19 software package to analyze the results and rank the technological parameters according to their degree of influence on the output characteristic of the process. The evaluation of how process parameters influence the microhardness is presented in Fig. 4.

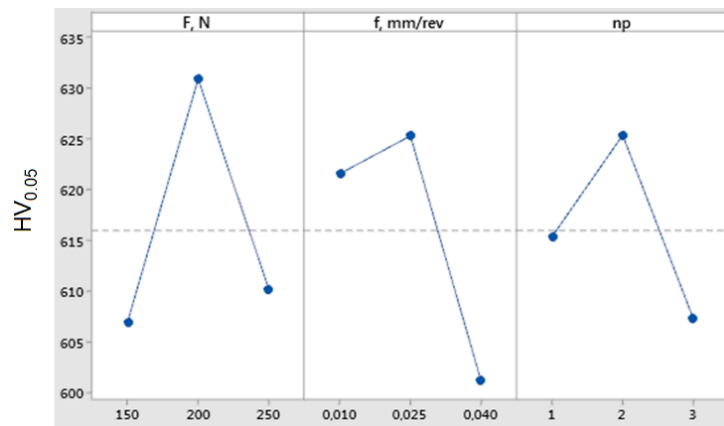


Fig. 4 Evaluation of how process parameters influence the output characteristic $HV_{0.05}$

We discovered that the tool feed rate has the most significant impact on the hardening of the surface layer. The optimal combination of technological parameters for hardening burnishing can be determined using the highest values of each parameter. Plots in Fig. 4 demonstrate that the optimal combination of the parameters based on microhardness $HV_{0.05}$ is a normal force of $F=200$ N, feed rate of $f=0.025$ mm/rev and number of passes $n_p=3$ (experiment 5). The microhardness value in this experiment was $657.4 HV_{0.05}$. Simultaneously, the average value of $Sa=73.35$ nm was slightly lower than the best value ($Sa=68.03$ nm) achieved in experiment 3. However, the microhardness of the surface area after burnishing with parameters $F=150$ N, $f=0.04$ mm/rev and $n_p=3$ (experiment 3) was only $595 HV_{0.05}$.

Using the optimal combination of technological parameters for burnishing established in experiment 5 yielded the results closest to the calculated values shown in Fig. 4.

The PSD analysis was used to evaluate the choice of burnishing parameter combination for reducing the influence of periodic impacts of the turning step. The assessment of PSD function was done for surfaces formed after hardening burnishing that used technological parameters according to experiments 3, 5, 7. For these studies, we used the technological parameter combinations with feed rates of 0.04, 0.025 and 0.01 mm/rev, and normal force values of 150, 200 and 250 N in three tool passes.

At the feed rate of $f=0.04$ mm/rev and the normal burnishing force of $F=150$ N, the PSD function value at spatial frequency $\omega_r=19.463$ mm⁻¹ was 176 nm²·mm, and at frequency ω_e PSD= 1129 nm²·mm (Fig. 5a). After reducing the feed rate to $f=0.025$ mm/rev and increasing the normal force to $F=200$ N in experiment 5, the PSD function had significantly lower values at both spatial frequency $\omega_r=19.463$ mm⁻¹ where PSD= 30.6 nm²·mm and at frequency $\omega_e=1.147$ mm⁻¹ where PSD= 991 nm²·mm (Fig. 5c). This indicates that the burnishing parameters adopted in experiment 5 minimize the influence of periodic impacts on the microprofile formation during the finish turning. After reducing the feed rate to $f=0.01$ mm/rev and increasing the burnishing force to $F=250$ N (experiment 7), the PSD function amplitude significantly increases at frequencies ω_e и ω_r to 31523 nm²·mm and 3293 nm²·mm (Fig. 5e). This mode significantly deteriorates the surface roughness, including to the point of destruction.

Reducing the feed rate f and increasing the normal force F during hardening burnishing increased the mean square deviation of surface irregularity height Sq from 86.05 nm after machining with parameters of experiment 3 (Fig. 5b) to 94.38 nm (experiment 5, Fig. 5d) and 610.24 nm (experiment 7, Fig. 5f).

Asymmetry of the Ssk profile, which is the measure of spatial deviations from the middle plane, increased from 0.36 (experiment 3) by about two times to 0.65 (experiment 5) and spikes quite significantly to 1.21 after the machining with technological parameters of experiment 7.

Thus, technological parameters of burnishing used in experiment 5 are optimal and essentially nullify the influence of periodic impacts seen during the turning of sample surfaces. Surfaces so obtained are best prepared for further technological transitions. So, the following machining transitions of deformation profiling of lubricating microcavities and smoothing burnishing were performed on samples after hardening burnishing with the following combination of technological parameters: $F=200$ N, $f=0.025$ mm/rev and $n_p=3$.

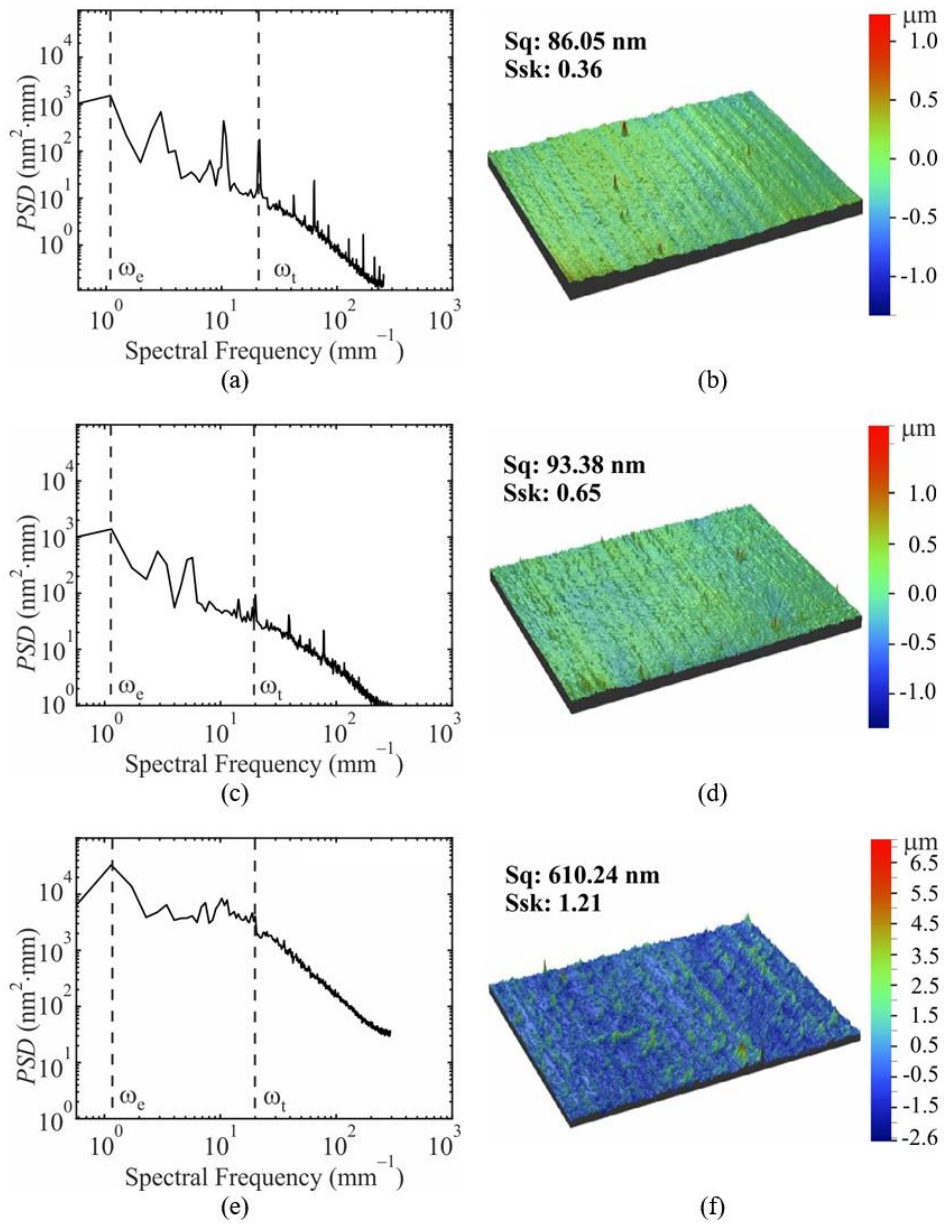


Fig. 5 PSD functions and sample surface topography after burnishing with parameter combinations used in experiments 3 (a, b), 5 (c, d) and 7 (e, f)

3.3. Deformation Profiling with The Honing Stone

Optimal honing stone grit parameters and application force were determined during the technological step of lubricating microcavity formation. The value of surface oil absorption power V_{vv} was maximized for this purpose. The deformation profiling of microcavities was carried out using honing stones with grit values of 160/125 and 200/250, with application force values F_p amounting to 200 and 250 N, providing for application pressure of 12.5 to 15.5 bar respectively for a 4×20 mm honing stone. Workpiece linear speed was set at 30 m/min. Similar parameters of nominally flat honing were used in [2].

Fig. 6a and b presents a 3D-topography and a profilogram of the surface after deformation profiling with the honing stone application force of $F_p=200$ N. The depth of microcavities obtained at $F_p=200$ N and the grit value of 160/125 was 1.7 to 5 μm . The height of formed microprotrusions was 1.8 μm to 4.5 μm . The oil absorption power of the surface after deformation profiling with the process parameters presented above $V_{vv}=18.47 \cdot 10^{-5} \text{ mm}^3/\text{mm}^2$ was determined using the MountainsMap software.

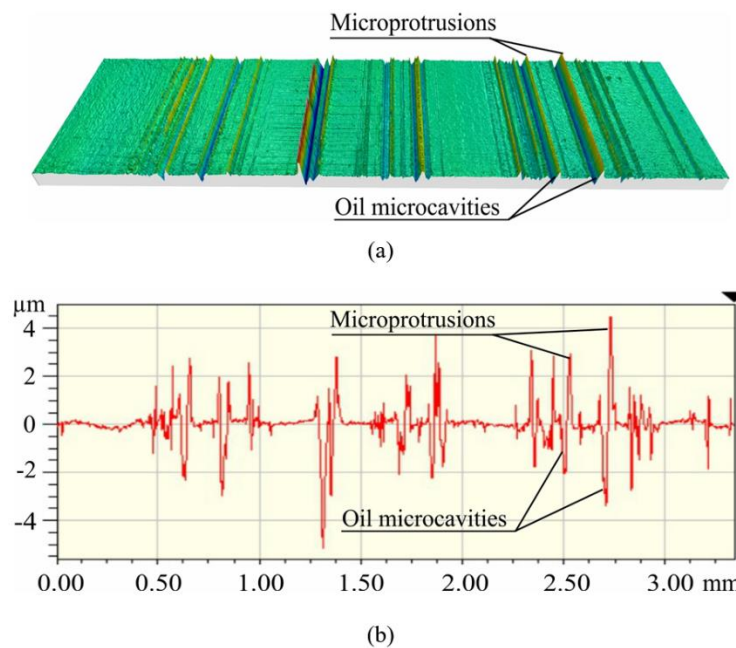


Fig. 6 3D-topography (a) and profilogram (b) of the surface after deformation profiling with the honing stone application force of $F_p=200$ N and the grit value of 160/125

The optimal parameters for deformation profiling were ultimately determined to be honing stone application force $F_p=250$ N and grit value of 200/250, which resulted in the microcavities with a depth from 3.8 to 8.1 μm . In this case, the oil absorption power of the surface reaches its maximal value $V_{vv}=59.07 \cdot 10^{-5} \text{ mm}^3/\text{mm}^2$ (Fig. 7a, b).

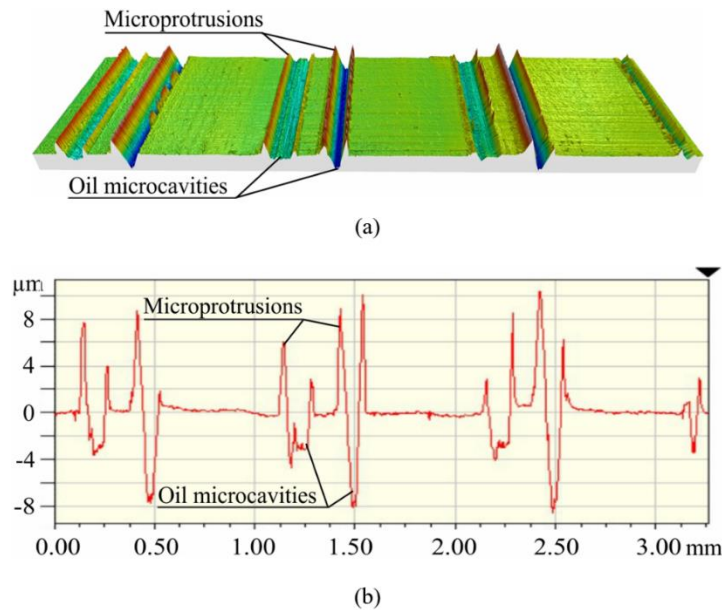


Fig. 7 3D-topography (a) and profilogram (b) of the surface after deformation profiling with the honing stone application force of $F_p=250$ N and the grit value of 200/250

3.4. Smoothing Burnishing

In the final step, we studied burnishing by a diamond indenter with the radius $R=6$ mm at two force values, 275 N and 300 N, seeking to remove microprotrusions and form a nominally flat surface while retaining the lubricating microcavities. Minimizing the parameter Sa and maximum microprofile peak deviation from the flatness FLTp [21] and maximizing the oil absorption power of the formed surface Vvv were taken as optimization criteria. Sa, FLTp and Vvv parameter values after smoothing burnishing are presented in Table 2.

Table 2. Flatness FLTp and oil absorption power Vvv values after smoothing burnishing

Surface parameters	Flatness and oil absorption power	
	$F_b=275$ N	$F_b=300$ N
Sa (nm)	244.8	149.7
FLTp (nm)	122.5	82.67
Vvv (mm^3/mm^2)	$10.76 \cdot 10^{-5}$	$13.74 \cdot 10^{-5}$

3D-topography and profilogram of the surface after smoothing with the normal force of $F_b=300$ N are shown in Fig. 8.

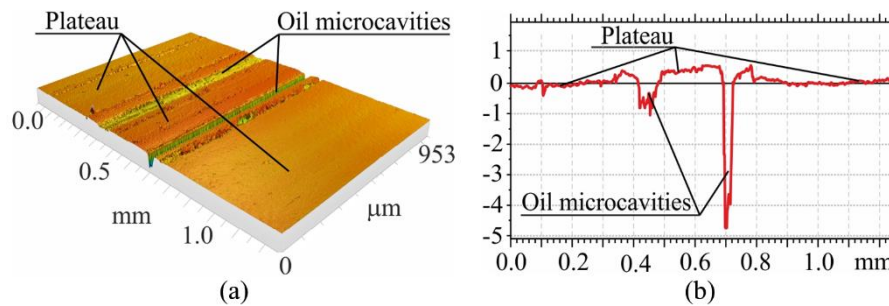


Fig. 8 3D-topography (a) and profilogram (b) of the surface after smoothing with the normal force of $F_b=300$ N

As can be seen from the above, the optimal smoothing burnishing force $F_b=300$ N yields the maximum surface oil absorption power $V_{vv}=13.74 \cdot 10^{-5} \text{ mm}^3/\text{mm}^2$ and minimum FLTp parameter: $\text{FLTp}=82.67$ nm. The mean absolute error of the microprofile amounted to $S_a=0.15 \text{ } \mu\text{m}$.

4. CONCLUSIONS

We carried out a series of studies relating to the formation of nominally flat surfaces with circumferential microcavities (grooves) on a shaft tribological assembly made of X38CrSi steel during multi-step machining on a turning center. This method of machining had been previously suggested by Nadolny and Kapłonek [7]. The initial data of the surface after finish turning were: mean absolute error of microprofile $S_a=440$ nm, microhardness $496 \text{ HV}_{0.05}$, oil absorption power $V_{vv}=6.95 \cdot 10^{-5} \text{ mm}^3/\text{mm}^2$. Also, PSD analysis of the surface topography revealed the influence of periodic frequencies ω_e and ω_f associated respectively with spindle speed $n=1650$ rev/min and turning feed $f=0.05$ mm/rev. The dominant influence of spatial frequency $\omega_e=1.147 \text{ mm}^{-1}$ is due to periodic impacts of the machine tool mechanical system in the region of low frequencies, multiple of the spindle speed.

Further study was aimed at determining the optimal parameters of technological steps of burnishing and deformation profiling of lubricating microcavities. Using the Taguchi L9 method of experiment planning, we established the relationship between the technological parameters of hardening burnishing (normal force, feed rate and number of tool passes) and microhardness $\text{HV}_{0.05}$ and the mean absolute error of the surface microprofile S_a . We discovered that normal burnishing force $F=200$ N, feed rate $f=0.025$ mm/rev and three tool passes are optimal and provide maximum hardening of the surface layer up to $657.4 \text{ HV}_{0.05}$ and nearly the minimum value of the mean absolute error of the microprofile $S_a=73.4$ nm.

The choice of the optimal combination of hardening burnishing parameters was assessed by the criterion of minimizing the influence of periodic impacts occurring at the preceding transition of finish turning by PSD-analysis. The PSD function amplitude was evaluated for surfaces formed after hardening burnishing with the best and worst parameters of microhardness $\text{HV}_{0.05}$ and roughness S_a . These surface topography parameters corresponded to burnishing feed rates of 0.04, 0.025, 0.01 mm/rev and normal forces of 150, 200 and 250 N at three tool strokes.

The best surface roughness $S_a=68$ nm was achieved at normal burnishing force $F=150$ N and feed rate $f=0.04$ mm/rev. The magnitude of PSD function amplitude at periodic frequency ω_e is 1035.5 nm²·mm and at frequency ω_t , the PSD function amplitude is 11.2 nm²·mm. However, the microhardness did not exceed 595 HV_{0.05} in that case.

It was discovered that when the feed rate is reduced to 0.01 mm/rev and the burnishing force is increased to 250 N, there is a significant increase in the amplitude of the PSD function to 3293 nm²·mm at periodic frequency ω_t and to 33182 nm²·mm at frequency ω_e . The mean absolute error of the microprofile increases to $S_a=440.1$ nm. We suspect that increasing normal force and decreasing feed rate aggravates the effect of machine tool mechanical system oscillations.

The established optimal parameters of hardening burnishing were used for surface preparation for subsequent transitions of deformation profiling of lubricating microcavities and final smoothing burnishing of microprotrusions.

Deformation profiling of lubricating microcavities was carried out by a special tool with a self-aligning honing stone. We revealed the relationship between the parameters of the honing stone grit, the force and pressure of its application against the surface with the depth of microgrooves and oil absorption power of the processed surface area.

It was established that the optimum parameters of deformation profiling are the honing stone grit of $200/250$ and the pressure of its application to the surface of 15.5 bar at the force 250 N. Machining with these parameters allowed us to obtain microcavities with depths from 3.8 to 8.1 μm and the oil absorption power of $V_{vv}=59.07 \cdot 10^{-5}$ mm³/mm². A similar level of microcavity depth and oil absorption power of tribological assembly surfaces had been obtained by other researchers [2-3].

Smoothing burnishing with a diamond indenter 6 mm in radius with normal force $F_b=300$ N and feed rate of $f=0.2$ mm/rev enabled us to practically eliminate microprotrusions after deformation profiling of lubricating microcavities. The mean absolute error of the microprofile amounted to $S_a=0.15$ μm. Simultaneously, due to reduction of the depth of lubricating microcavities to $1.7...4.1$ μm the oil absorption power of the surface sank to $13.74 \cdot 10^{-5}$ mm³/mm². After the deformation profiling and flat-top burnishing steps, the microhardness of the bearing area decreased to 605 HV_{0.05}. This is due to the surface de-hardening after honing.

At the optimum mode of preliminary strengthening burnishing at force $F=200$ N and feed rate of $f=0.025$ mm/rev, the parameters of the surface PSD amplitude function increased insignificantly and amounted to 30.6 nm²·mm at ω_t and 1386.9 nm²·mm at ω_e , respectively.

For further optimization, assistance of burnishing by ultrasonic oscillations may be considered [22], as well as application of coatings [23].

Acknowledgement: *Funding from the Ministry of Science and Higher Education of the Russian Federation (Ural Federal University, the State Assignment № 075-03-2023-006 of 16.01.2023 (FEUZ-2024-0020)) is acknowledged.*

REFERENCES

1. Pawlus, P., Reizer, R., Wieczorowski, M., 2021, *Analysis of surface texture of plateau-honed cylinder liner - A review*, Precision Engineering, 72, pp. 807-822.
2. Koszela, W., Pawlus, P., Rejwer, E., Ochwat, S., 2013, *Possibilities of oil pocket creation by the burnishing technique*, Archives of civil and mechanical engineering, 13(4), pp. 465-471.
3. Mezghani, S., Demirci, I., Yousfi, M., Mansori, E.M., 2013, *Running-in wear modeling of honed surface for combustion engine cylinder liners*, Wear, 302(1-2), pp. 1360-1369.
4. Zhang, Y.K., Yang, C.J., Fu, Y.H., Zhou, J.Z., Hua, X.J., Ji, J.H., 2008, *Surface texturing technology by laser honing based on hydrodynamic lubrication*, Key Engineering Materials, 359-360, pp. 340-343.
5. Molnár, V., 2022, *Tribological properties and 3D topographic parameters of hard turned and ground surfaces*, Materials, 15(7), 2505.
6. Molnár, V., 2022, *Wear resistance of hard turned surfaces*, Cutting and Tools in Technological System, 96, pp. 65-72.
7. Nadolny, K., Kapłonek, W., 2014, *Analysis of flatness deviations for austenitic stainless steel workpieces after efficient surface machining*, Measurement Science Review, 14(4), pp. 204-212.
8. Kuznetsov, V.P., Makarov, A.V., Psakhie, S.G., Savrai, R.A., Malygina I.Yu., Davydova N.A., 2014, *Tribological aspects in nanostructuring burnishing of structural steels*, Physical Mesomechanics, 17, pp. 250-264.
9. Patel, N.S., Parihar, P.L., Makawana, J.S., 2021, *Parametric optimization to improve the machining process by using Taguchi method: a review*, Materials Today: Proceedings, 47(11), pp. 2709-2714.
10. Sakthivelu, S., Anandaraj, T., 2017, *Prediction of optimum machining parameters on surface roughness and MRR in CNC drilling of AA6063 alloy using design of experiments*, International Journal of Engineering Research & Technology, 5 (13), pp. 1-5.
11. Krishnaprakasha, P., Pavitra, A., 2018, *Optimization of drilling parameters on surface roughness of Al 1200-SiC composites using Taguchi analysis*, IOSR Journal of Mechanical and Civil Engineering, 15(3), pp. 77-84.
12. Patel, R., Patel, S., Patel, P., Parmar, P., Vohra, J., 2021, *Optimization of machining parameters for En8D carbon steel by Taguchi orthogonal array experiments in CNC turning*, Materials Today: Proceedings, 44(1), pp. 2325-2329.
13. Kuznetsov, V.P., Dmitriev, A.I., Anisimova, G.S., Semenova, Yu.V., 2016, *Optimization of nanostructuring burnishing technological parameters by Taguchi method*, IOP Conference Series: Materials Science and Engineering, 124, 012022.
14. Kuznetsov, V.P., Gorgots, V.G., Vorontsov, I.A., Skorobogatov, A.S., Kosareva, A.V., 2023, *Surface hardening of medical parts made of AISI 304 austenitic stainless steel by nanostructuring burnishing*, AIP Conference Proceedings, 2899, 020085.
15. Jacobs, T., Judge, T., Pastewka, L., 2017, *Quantitative characterization of surface topography using spectral analysis*, Surface Topography: Metrology and Properties, 5, 013001.
16. Peresadko, A.G., Hosoda, N., Persson, B.N.J., 2005, *Influence of surface roughness on adhesion between elastic bodies*, Physical Review Letters, 95, 124301.
17. Pohrt, R., Popov, V.L., 2012, *Normal contact stiffness of elastic solids with fractal rough surfaces* Physical Review Letters, 108, 104301.
18. Popov, V.L., Pohrt, R., 2018, *Adhesive wear and particle emission: Numerical approach based on asperity-free formulation of Rabinowicz criterion*, Friction, 6, pp. 260-273.
19. Žak, K., 2018, *Fractal and frequency based analysis of rough surfaces produced by different machining operations on hardened alloy steel parts*, Advances In Manufacturing Science And Technology, 42(1-4), pp. 43-53.
20. Martins, A.M., Oliveira, D.A., de Castro Magalhães, F., Abrão, A.M., 2023, *Relationship between surface characteristics and the fatigue life of deep rolled AISI 4140 steel*, The International Journal of Advanced Manufacturing Technology, 129, pp. 1127-1143.
21. International Organization for Standardization, 2003, *Geometrical Products Specifications (GPS) – Flatness – Part 1: Vocabulary and parameters of flatness*. ISO/TS 12781-1:2003.
22. Popov, M., 2021, *Friction under large-amplitude normal oscillations*, Facta Universitatis-Series Mechanical Engineering, 19(1), pp. 105-113.
23. Zinoviev, A., Balokhonov, R., Zinovieva, O., Romanova, V., 2022, *Computational parametric study for plastic strain localization and fracture in a polycrystalline material with a porous ceramic coating*, Mechanics of Advanced Materials and Structures, 29(16), pp. 2390-2403.